16th World Conference on Earthquake Engineering, 16WCEE 2017

Santiago Chile, January 9th to 13th 2017

Paper N° 2849

Registration Code: S-D1466049490

ANALYTICAL ESTIMATE OF NONLINEAR MATERIAL PARAMETERS FOR MASONRY STRUCTURES UNDER LATERAL LOADS

N. R. Peralta(1) and K. M. Mosalam(2)

(1) *Ph.D candidate, University of California, Berkeley, n.peralta@berkeley.edu*

(2) *Taisei Professor of Civil Engineering and Director of PEER, University of California, Berkeley, mosalam@berkeley.edu*

Abstract

The theory of micromechanical homogenization is used for the prediction of effective material properties for the use in macroscopic nonlinear simulations of masonry structures subjected to lateral loads, e.g. due to seismic loads, using a well-established model such as the total strain rotating crack (TSRC) model. The mechanical and geometrical properties of the constituents (mortar joints and brick units) are explicitly considered in a detailed microscopic three-dimensional (3D) finite element (FE) model of a typical masonry unit cell subjected to a monotonically increasing state of macro strain. The macro stress history is obtained so that a macroscopic stress-strain relationship is established for a particular orientation of principal strains. The effective parameters for nonlinear analysis are selected based on the obtained stress-strain curve. This set of effective parameters is used in a macroscale model to test their ability in replicating full micro analytical modeling as well as experimental results of full-scale specimens. The proposed homogenized model is suitable for an efficient computation of the nonlinear behavior of masonry structures where experimental results are unavailable. On the other hand, it is also suitable for parameters determination for masonry structures subjected to complex state of stresses as the case of a masonry wall containing openings and/or complicated geometric/loading conditions. Such a parametric model can also serve as a key component for the analytical estimation of the seismic vulnerability of systems containing masonry components, e.g. masonry structures and infilled frames, for subsequent reliability-based performance-based earthquake engineering applications.

Keywords: Micromechanics; homogenization; masonry structures; nonlinear analysis.

1. Introduction

Masonry is a construction material used in most of old buildings around the world as well as in many of the modern buildings especially in developing countries. It typically consists of a manual arrangement of individual units, e.g. bricks or stones, bonded together by mortar joints. This arrangement can be random, as observed in most heritage buildings. On the other hand, the arrangement can be organized in a periodic fashion as observed in most modern buildings. In both cases, the response of such structures depends on the properties of the two constituting phases and their spatial distribution (as characterized by their arrangement and the size of each of them). Masonry is thus a heterogeneous material but, in most structural analysis and design, masonry is considered as a homogeneous material with effective parameters in terms of stiffness and strength. The analysis and design of new masonry structures as well as the vulnerability analysis and retrofit of existing ones require an appropriate selection of the effective parameters.

In the current state of structural and earthquake engineering, it is obvious that physical simulations provide the most suitable venue to gain a better understanding of the behavior of structural components and systems. The effective parameters needed for a large-scale numerical simulation of masonry structures can be inferred from the observed behavior obtained by physical experimentation. However, physical, economical and time constraints restrict the versatile employment of the experimental simulations. In contrast, analytical simulations possess significantly smaller amount of physical and economical constraints and they provide increased accuracy with the increased model size and sophistication and corresponding simulation duration.

Many studies are found in the literature for the determination of the effective elastic constants for masonry structures. Most of these studies rely on the theory of micromechanical homogenization. The reader is referred to [1], [9], [10], [19], [21], [23], [24], etc. However, limited work is available in the literature for the analytical prediction of the strength and full nonlinear behavior of masonry structures subjected to complex states of stress or deformation. Based on experimental observations on masonry walls subjected to loads in different orientations, Lourenço (1996) [15] developed a plasticity model for masonry in which Hill criterion was adopted for compressive strength while Rankine criterion was adopted for tensile strength. Berto et al. (2002) [8] developed an orthotropic damage model for masonry accounting for the stiffness recovery of masonry upon crack closure. Their model was tested against experiments and good analytical versus experiment agreement was observed. Kawa et al. (2008) [12] used lower bound theory of plastic analysis for the determination of limit stress of a masonry unit cell. They assumed Mohr-Coulomb failure criterion for both mortar joint and brick units. This process involves a constrained optimization problem over all possible admissible stress fields for the determination of strength in a particular orientation. Luciano and Sacco ([14] and [15]) developed a micromechanical damage model for masonry structures by homogenizing the undamaged and damaged state of masonry. They assumed that damage concentrates on mortar joints and that bricks remain elastic. Zucchini and Lourenço (2009) [25] combined a damage model in tension with a plasticity model in compression. The classical computational homogenization was used, and Drucker-Prager plasticity was assumed for each phase with the return mapping algorithm for the computation of plastic strains. They show the capability of the computational homogenization in replicating results from a meso-scale modeling of masonry.

In a recent publication, [20], the authors developed a two-dimensional (2D) computational micromechanical model, based on the finite element method (FEM), for masonry structures. Effective elastic constants were obtained using the classical computational homogenization technique [13] and the asymptotic homogenization [22], Both methods led to the same results. The homogenized elastic parameters were used on macroscale simulation of specimens for which experimental results were available and they were observed to be in an acceptable agreement. A similar model is presented herein but in three-dimensions (3D). Furthermore, nonlinear properties are considered for each phase as well as for their interface. This model is expected to account for the different modes of failure of masonry including vertical splitting cracks in brick units as a result of the tensile force exerted by mortar joints in the out of plane direction of the splitting plane.

The study of the strength properties of masonry structures is undoubtedly important not only for the analysis and design of new masonry structures but also for evaluating and accordingly retrofitting existing and heritage masonry structures. Drawbacks of the physical experimentations of masonry walls are not only limited to resources limitations but also to the fact that structural response of such structures is highly dependent of the characteristics of the state of stress (i.e. direction of principal stresses) and also the characteristics of the primitive cell, including but not limited to the topology (which typically varies significantly especially from heritage buildings to modern ones), thickness of joints, phase material type and quality, etc. This makes specific experimental results applicable to very limited cases and extrapolation to different scenarios might not be straightforward. Thus, having a robust way of characterizing the macroscopic properties of masonry is essential.

In this paper, we start by presenting some experimental results on masonry walls. Then, we describe the homogenization approach and finally, we discuss the comparison of results between the proposed analytical model and the experiments.

2. Experiments on masonry walls

Masonry is a complex composite of bricks and mortar joints. The behavior of a masonry wall depends on the properties of the brick units, the mortar joints, and the mortar-brick interfaces. Several tests, discussed in this section, of materials used in the construction of panels were conducted to understand the wall panel behavior.

2.1 Brick units

Clay bricks have dimensions 3-5/8 × 2-1/4 × 7-5/8 in. The bricks compressive strength was determined by testing five bricks in accordance with ASTM C 67 [1]. The bricks were saw cut in half, capped and loaded perpendicular to the bed joint. Unlike the ASTM standard, the bricks were not dried so that the strength value was representative of conditions in the wall panels. Moreover, the bricks were not shellacked, but were capped with hydrostone. Compressive strength was determined as

$$C = W/A \tag{1}$$

where W is the maximum load and A is the gross cross-sectional area perpendicular on the loading direction. For tensile strength, each brick is loaded perpendicular to the bed joint via a long metal rod that lies across the brick in accordance with ASTM C 1006 [3]. The splitting tensile strength, T, was determined using

$$T = 2P/\pi LH \tag{2}$$

where P is the maximum applied load, L is the net split length, and H is the brick height. The test creates a nearly constant tensile stress that results in strength values that are slightly higher than the direct tension tests [11] .

The bricks modulus of rupture is related to the bricks tensile strength. This test was conducted in accordance with ASTM C 67 [1], except that the five brick units were not dried so that the strength value was representative of conditions in the wall panels. ASTM calculates the modulus of rupture, S, as

$$\mathrm{S} = 3W(L/2 - x)/bd^2 \tag{3}$$

where W is the maximum applied load, L is the span length, b is the net width, d is the brick height, and x is the average distance from the mid-span of the specimen to the plane of failure measured in the direction of the span along the centerline of the bed surface subjected to tension. Tensile strength value (516 psi) was determined from the split tension test. The arching action and the fact that a smaller fraction of the section is being highly stressed, explain why the average modulus of rupture value (794 psi) is significantly greater than the average tensile strength value (516 psi) determined from the split tension test. The average distance, x, from the mid-span of the specimen to the plane of failure was as large as 1-1/16 in. This large value demonstrates that small flaws can greatly influence the brick strength were failure does not always occur at the cross-section with the largest bending moment. This is supported by the large COV (25%) where bricks generally failed in a brittle manner with a single visible crack near the center. However, one brick lost its load carrying capacity in a rather ductile manner with no visible cracks. According to the modulus of rupture tests, the brick net tensile strength was about 18% of the net compressive strength.

2.2 Mortar joints

Mortar cylinders were cast for compression and split tension tests. The cylinders were 3 in. diameter and 6 in. long. They were compacted with a rod after each third of the cylinder was placed and were further consolidated with a vibration table. The cylinders were tested according to ASTM C 496 [4] after 7 days of curing in a fog room. A set of split-tension tests were performed in which the cylinders were subjected to a compressive load parallel to the longitudinal axis of the cylinder. The compressive strength of the mortar was determined according to ASTM C 39 [5] in which the cylinders were loaded axially.

2.3 Masonry Direct shear tests

Direct shear tests were performed with the same bricks and mortar using four brick assemblies. A load, P, was applied to the center bricks in parallel to bed joints and the gross shear stress was calculated as

$$\tau = 0.5P/A_g \tag{4}$$

where A_g was 12.7 in^2.

2.4 Masonry prism test

Five prisms where each prism consisted of three units stacked on top of each other, and bonded together by mortar joints were tested in compression according to ASTM E 447 [6]. The prisms were cured 21 days in the fog room followed by 7 to 8 days at room temperature before testing. The specimens were loaded at a rate of about 55 kips per minute. The average compressive strength was 2.906 ksi with a COV of 4%.

2.5 Masonry constituents test results

Table 1 summarizes the results of the previously discussed experiments.

Table 1 – Masonry component test results

Test	Curing (days)	# of Specimens	Average Strength (ksi)	COV
Brick Compression	-	5	4.341	24%
Modulus of Rupture	-	5	0.794	25%
Brick Split Tension	-	4	0.516	18%
Mortar Compression	7	3	0.736	2%
	28	3	1.179	2%
Mortar Split Tension	7	3	0.113	9%
	28	3	0.186	3%
Comp. Masonry Prism	28	5	2.906	4%
Masonry Shear	-	2	0.106	5%

2.6 Diagonal tension test of a masonry wall

The diagonal tension test of masonry walls is performed to study the behavior of the walls when subjected to a state of stress dominated by shearing. Fig. 1 shows the applicability of such test.

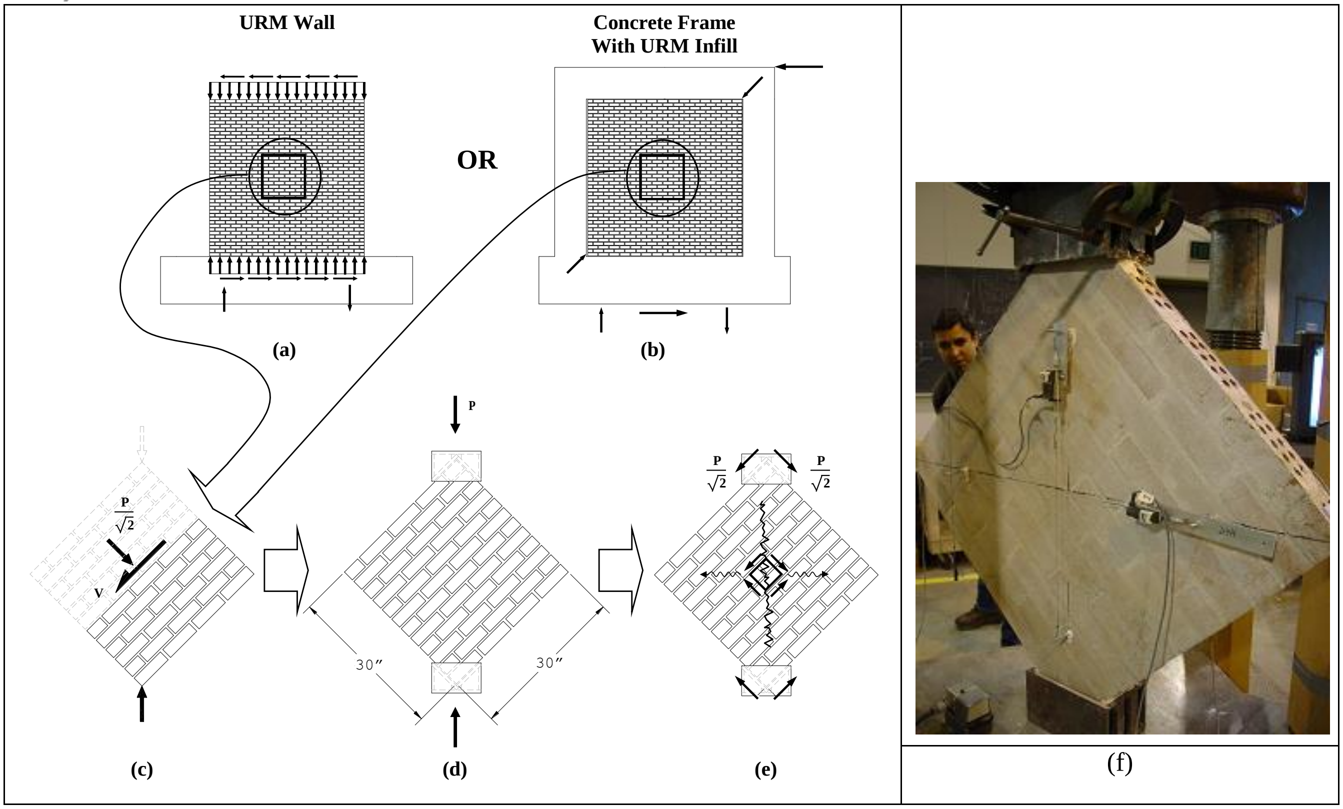

Fig. 1 – (a) Unreinforced masonry (URM) wall; (b) Concrete frame with URM infill; (c) Free body diagram of a panel; (d) Schematic representation of diagonal tension test setup; (e) State of stress inducing diagonal tension at the center of the wall; (f) Picture of diagonal tension test [17]

2.6.1 Test setup

30 in.×30 in. square panels were constructed in the pattern shown in Fig. 1(d) with half blocks at every other row end. Vertical and horizontal joints were approximately 9/32 in. The test was performed according to ASTM E 519 [7]. To create the loading condition shown in Fig. 1 (d), the panel corners were capped with hydrostone and placed into steel loading shoes. The placement was checked carefully to ensure that the wall was vertically plumb and loading shoes were placed evenly. The panel was subjected to monotonic quasi-static loading at an average rate of 6.6 kips per minute. The loading rate was calculated by dividing the load at yield by the time to yield. After placing the panels in the test machine, small holes were drilled into the brick on each side of the panel near the corners where tension and shear stresses would be small. Threaded rods were inserted into the holes and embedded with hydrstone. Displacement transducers were placed on the rods to measure horizontal and vertical displacements on each side of the specimen. Inserting the rods into the brick had minimal effect since cracks never initiated in the vicinity of the rods. Another displacement transducer measured the displacement of the loading head and a load cell measured the applied force.

2.6.2 Results

Fig. 2 depicts the shear force versus drift relationship, where the shear force is normalized by the wall original thickness as follows:

$$V/t = P/t\sqrt{2} \tag{4}$$

where t is the thickness of the wall and P is the applied load. From Fig. 1(c), it is clear that the bricks near the center of the panel experience compressive and shearing action. In an URM wall, axial load would develop due to gravity, overturning moment, and/or vertical ground acceleration, whereas the shear load would be transferred to the wall from the inertia effects of floor or roof diaphragms, Fig. 1(a). The wall drift, δ, is based on

$$\delta = \left(L - \sqrt{\left(\sqrt{2}L - \Delta_u\right)^2 - L^2}\right)/L \tag{5}$$

where L is the average gage length of the two vertical displacement transducers and Δ_u is the average of the magnitude change in length of each vertical gage. The drift equation is only an approximation of the actual panel deformation. The equation assumes that the length of each panel edge remains constant and that the wall shortens vertically the same amount that the wall expands horizontally. The latter assumption is not entirely accurate since displacement transducers indicate that the vertical and horizontal displacements are not of the same magnitude especially at large displacements, but on average the above equation gives a reasonable estimate of the performance of a brick panel.

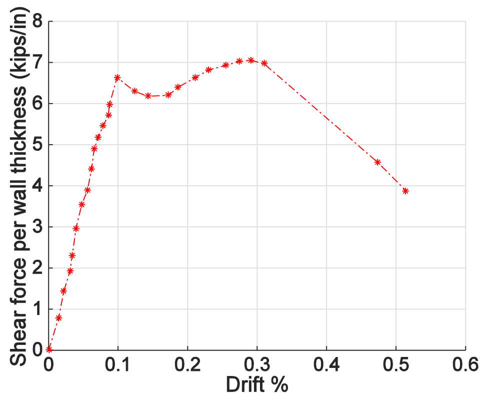

Fig. 2 – Masonry wall diagonal tension test results

3. Computational homogenization

3.1 Masonry unit cell

Although the concept of unit cell is often confused with that of a representative volume element in statistically homogeneous solids, for periodic microstructure we use the unit cell to refer to the primitive cell that contains all geometric and mechanical features of the microstructure. In principle, one should be able to generate a full micro structural model of a large scale system by replicating the unit cell. Thus, the size of the unit cell is related to the periodicity of the micro structure. Fig. 3 shows the FE mesh of a masonry unit cell.

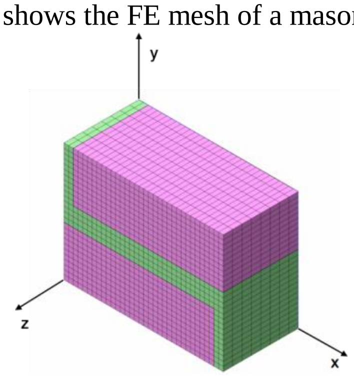

Fig. 3 – Finite element mesh of masonry unit cell

Micromechanical homogenization aims to find overall behavior of large-scale heterogeneous solids by relating it to the behavior of the unit cell. We perform analysis on this masonry unit cell to obtain the overall effective material properties to be used in large scale simulations. Each phase (mortar and brick) is given its corresponding material and geometrical properties. We assume the following mechanical properties (modulus of elasticity, E_c, Poisson's ratio, v, compressive strength, f_c, tensile strength, f_t, compressive fracture energy, G_c, and tensile fracture energy, G_t) for brick and mortar joints. Note that fracture energy is energy dissipated during formation of a unit area of damage in compressive crushing or tensile fracture. It is the area under the stress-strain relationship multiplied by an intrinsic length scale and is treated as a material property (Mosalam and Paulino, 1997) [18]

Table 2 – Material properties for the FE simulation

	$\mathbf{E_c}$ (ksi)	v	$\mathbf{f_c}$ (ksi)	$\mathbf{f_t}$ (ksi)	$\mathbf{G_c}$ (kips.in)	$\mathbf{G_t}$ (kips.in)
Brick Units	1595.0	0.15	4.34	0.60	0.003	0.000088
Mortar Joints	320.0	0.25	1.18	0.19	0.001	0.000050

3.2 Homogenization approach

If we impose constant unit increments of strain, $d\mathbf{E}_{kl}$, in each direction, the stress increments, $d\mathbf{\Sigma}_{ij}$, correspond to the effective coefficients of the tangent material moduli at a particular state of strain, $\mathbb{C}^{eff}_{ijkl}$, i.e.

$$\mathbb{C}^{eff}_{ijkl} \coloneqq d\mathbf{\Sigma}_{ij} \quad \text{due to unit constant} \quad d\mathbf{E}_{kl} \tag{7}$$

In 3D general problems, for each unit component of strain increments, we obtain 9 stress components. Since we repeat this process for the 9 strain components, we obtain 81 components to fill the 9×9 matrix of material moduli. In most applications, symmetry of such matrix reduces the number of independent material moduli. However, it is important to observe that heterogeneous material does not necessarily preserve the same material symmetry of their phase components. The components of $d\Sigma_{ij}$ are obtained by averaging the stresses in the unit cell subjected to the following boundary (∂V) conditions:

$$u_i(x) = \mathbf{E}_{ij} \cdot x_j\,, \;\; \forall\, x_j \in \partial V \tag{8}$$

where $\mathbf{E}_{ij}$ is a constant strain. In 2D problems, we impose the following constant strain conditions:

$$\text{Case a:} \;\; \text{unit } \mathbf{E}_{xx} = \begin{bmatrix} 1 & 0 \\ 0 & 0 \end{bmatrix} \qquad \text{Case b:} \;\; \text{unit } \mathbf{E}_{yy} = \begin{bmatrix} 0 & 0 \\ 0 & 1 \end{bmatrix} \qquad \text{Case c:} \;\; \text{unit } \mathbf{E}_{xy} = \begin{bmatrix} 0 & 1 \\ 1 & 0 \end{bmatrix} \tag{9}$$

3.3 Homogenization for elastic parameters

The unit cell is subjected to the three cases in Eqs. (9). The solution is shown in Figs. 4 to 7.

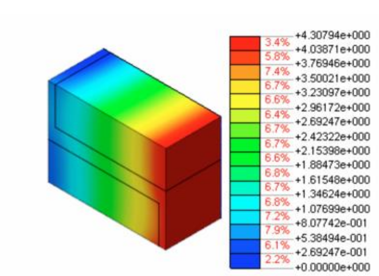

Case a. Constant Strain E_{xx}

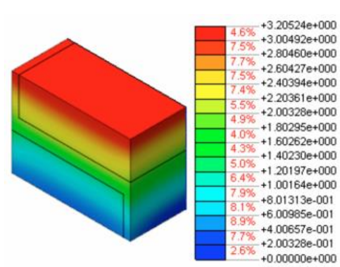

Case b. Constant Strain E_{yy}

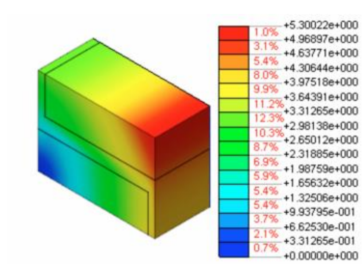

Case c. Constant Strain E_{xy}

Fig. 4 – Displacement field of the masonry cell (inches, % elements within the specified displacement range)

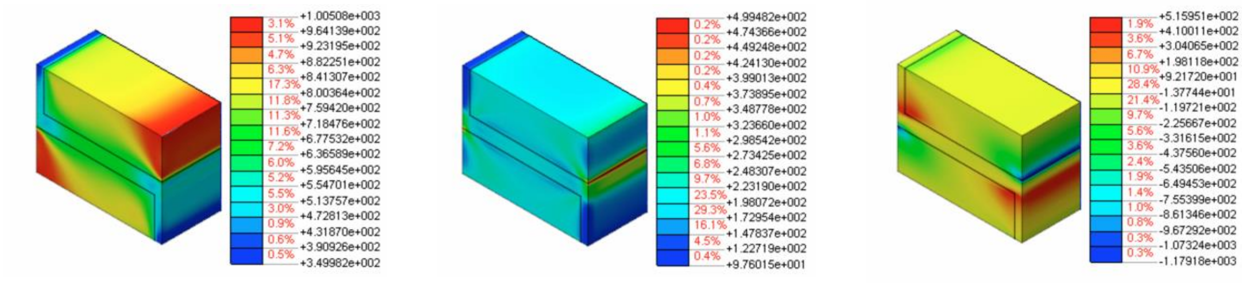

Case a Case b Case c

Fig. 5 – σ_{xx} distribution (ksi, % of elements within the specified stress range)

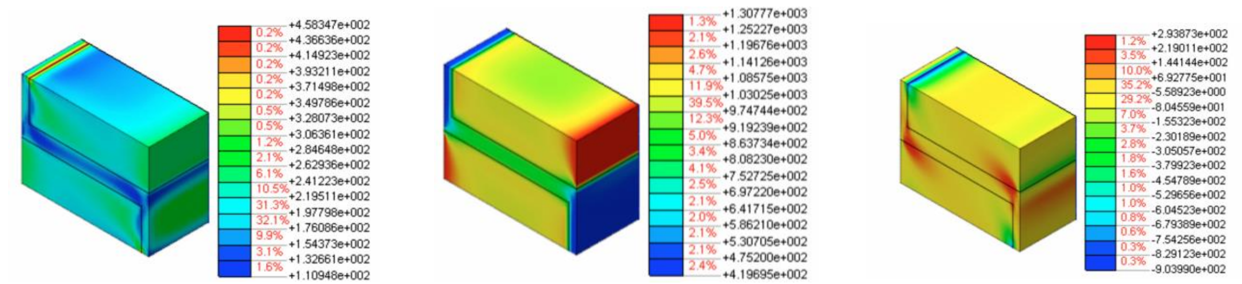

Case a Case b Case c

Fig. 6 – σ_{yy} distribution (ksi, % of elements within the specified stress range)

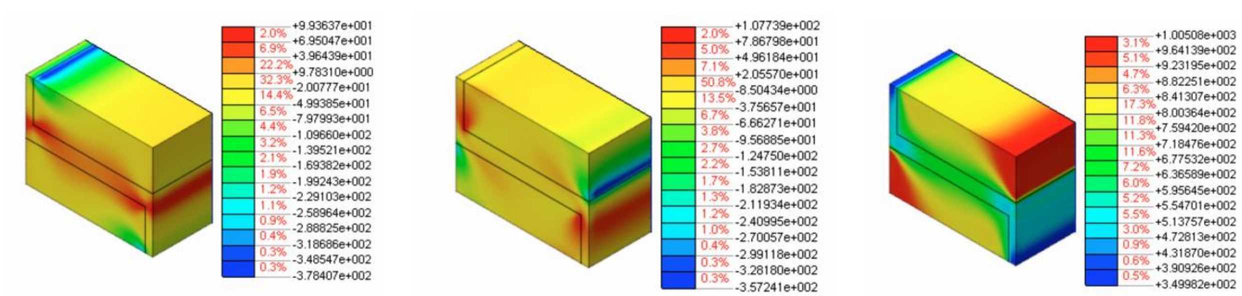

Case a Case b Case c

Fig. 7 – σ_{xy} distribution (ksi, % of elements within the specified stress range)

Each finite element in the mesh depicted in Fig. 3 belongs to either a brick or mortar phase. Stresses are computed for each element using the appropriate constitutive relationship for each phase. We obtain three stress fields (σ_{xx}, σ_{yy}, and σ_{xy}) for each of the applied macro strain cases shown in Eqs. (9). The resulting nine stress distributions are shown in Figs. 5-7. By definition, the weighted average of each of the obtained stress distributions, for each element gives the following material moduli:

$$[C^{\mathrm{Masonry}}] = \begin{bmatrix} \mathbb{C}_{1111} & \mathbb{C}_{1122} & \mathbb{C}_{1112} \\ \mathbb{C}_{2211} & \mathbb{C}_{2222} & \mathbb{C}_{2212} \\ \mathbb{C}_{1211} & \mathbb{C}_{1222} & \mathbb{C}_{1212} \end{bmatrix} = \frac{1}{V_{unit\ cell}} \left(\sum_{n=1}^{nel} (\sigma_{\mathrm{ij}} \text{ due to unit } \epsilon_{\mathrm{kl}}) \cdot V_n \right)$$
$$= \begin{bmatrix} 1067 & 200 & -1.015 \\ 200 & 975 & -0.580 \\ -1.015 & -0.580 & 381 \end{bmatrix} \text{ ksi} \tag{10}$$

where *nel* is the number of elements, $V_{unit\ cell}$ is the volume of the unit cell and V_n is the volume of the n^{th} finite element. According to the above results, masonry can be idealized as an orthotropic material (material directions 1 and 2) with the effective properties listed in Table 3, where G is the shear modulus.

Table 3 – Effective material properties

Parameter	$\mathbf{E_{11}}$ (ksi)	$\mathbf{E_{22}}$ (ksi)	$\boldsymbol{v_{12}}$	**G** (ksi)
Value	1026.0	946.9	0.21	381.0

4. Nonlinear FE model of masonry cell

We analyze the unit cell subjected to monotonically increasing strains and the following boundary conditions:

$$\mathrm{u_i}(x, \epsilon_{yy}) = \left[\mathbf{E}_{yy}(\epsilon)\right]_{\mathrm{ij}} \cdot x_{\mathrm{j}}, \qquad \mathrm{u_i}(x, \epsilon_{xx}) = [\mathbf{E}_{xx}(\epsilon)]_{\mathrm{ij}} \cdot x_{\mathrm{j}} \qquad \forall\, x\, \in \partial\mathrm{V} \tag{11}$$

where

$$\mathbf{E}_{yy}(\epsilon) = \begin{bmatrix} 0 & 0 \\ 0 & \epsilon \end{bmatrix} \quad \text{and} \quad \mathbf{E}_{xx}(\epsilon) = \begin{bmatrix} \epsilon & 0 \\ 0 & 0 \end{bmatrix} \tag{12}$$

The stress vs strain relationship for each case is shown in Fig. 8

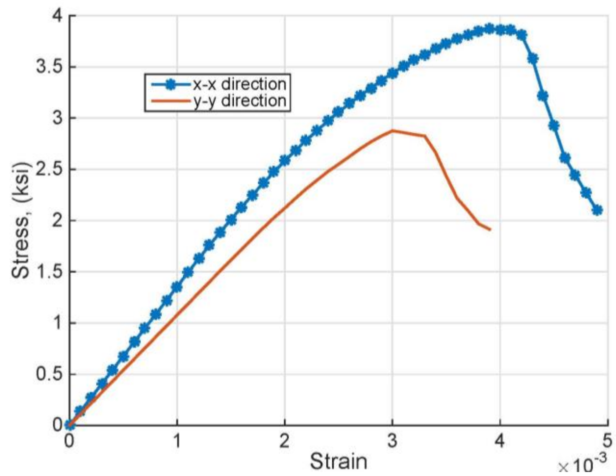

Fig. 8 –Stress vs strain for masonry unit cell

4.1 Analysis of rotated unit cell

The unit cell is subjected to state of strain in arbitrary direction via macro strain transformation. We subject the unit cell to the following boundary condition:

$$\mathrm{u_i}(x, \epsilon, \theta) = [\mathbf{E}_{x'x'}(\epsilon, \theta)]_{\mathrm{ij}} \cdot x_{\mathrm{j}}, \qquad \forall\, x\, \in \partial\mathrm{V} \tag{13}$$

where

$$\mathbf{E}_{x'x'}(\epsilon, \theta) = [\mathbf{Q}(\theta)][\mathbf{E}_{xx}(\epsilon)][\mathbf{Q}(\theta)]^{\mathrm{T}} \tag{14}$$

and $\mathrm{Q}(\theta)$ is a rotation operator given by

$$\mathbf{Q}(\theta) = \begin{bmatrix} \cos\theta & \sin\theta \\ -\sin\theta & \cos\theta \end{bmatrix} \tag{15}$$

When we average the stress field due to $\mathbf{E}_{\mathrm{x'x'}}(\epsilon, \theta)$, we need to rotate it back to the inclined plane, then

$$\mathbf{\Sigma}_{\mathrm{i'j'}}(\epsilon,\theta) = [\mathbf{Q}(\theta)]^{\mathrm{T}} \left(\frac{1}{V_{unit\ cell}} \left(\sum_{n=1}^{nel} (\sigma \text{ due to } \mathrm{E}_{x'x'}(\epsilon,\theta)\,) \cdot V_n \right) \right) [\mathbf{Q}(\theta)] \tag{16}$$

As an example, we are analyzing the unit cell rotated 45^{o} by imposing the following state of strain:

$$\mathbf{E}_{\mathrm{x'x'}}(\epsilon, 45^{\mathrm{o}}) = [\mathbf{Q}(45^{\mathrm{o}})][\mathbf{E}_{\mathrm{xx}}(\epsilon)][\mathbf{Q}(45^{\mathrm{o}})]^{\mathrm{T}} = \begin{bmatrix} 0.5 & -0.5 \\ -0.5 & 0.5 \end{bmatrix} \epsilon \tag{17}$$

Accordingly, the longitudinal stress at this orientation is given by the following:

$$\mathbf{\Sigma}_{x'x'}(\epsilon, 45^{\mathrm{o}}) = \left(\mathbf{\Sigma}_{xx} + \mathbf{\Sigma}_{yy}\right)/2 - \mathbf{\Sigma}_{xy} \tag{18}$$

4.2 Unit cell subjected to fields with moderate tensile strain

Up to this point, the strain fields we have analyzed are uniaxial producing the Mohr circle in Fig. 9a where we have analyzed the unit cell for a longitudinal strain in a particular orientation, zero strain in the orthogonal direction and zero force boundary condition in the *z-z* direction. Herein, we are analyzing the unit cell subjected to fields with moderate tensile strain in the orthogonal direction (Fig. 9b) to the applied strain to subject the unit cell to the expected state of strain in a diagonal tension test specimen. Elastic analysis of a masonry wall under diagonal tension, using the elastic parameters in Table 2 suggests that the center of the wall is subjected to horizontal strain of about 40% of the vertical strain. Thus, we analyze the unit cell subjected to the state of strain shown in Eqs. (19). The stress vs strain relationship in this case is shown in Fig. 10.

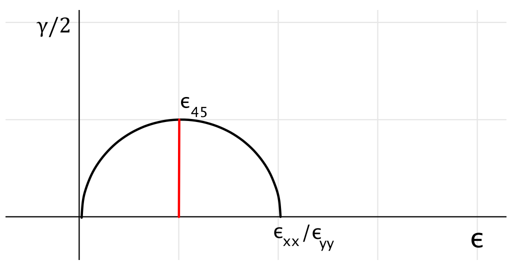

a. Uniaxial strain

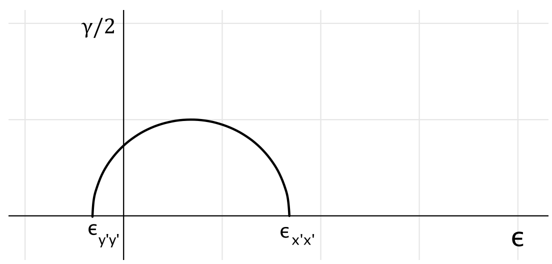

b. Fields with moderate tensile strain

Fig. 9 – Mohr circle representation of imposed strains

$$\mathbf{E}_{x'x'}(\epsilon, 45^{\mathrm{o}}) = [\mathbf{Q}(45^{\mathrm{o}})] \begin{bmatrix} 1 & 0 \\ 0 & -0.4 \end{bmatrix} \epsilon [\mathbf{Q}(45^{\mathrm{o}})]^{\mathrm{T}} = \begin{bmatrix} 0.3 & -0.7 \\ -0.7 & 0.3 \end{bmatrix} \epsilon \tag{19}$$

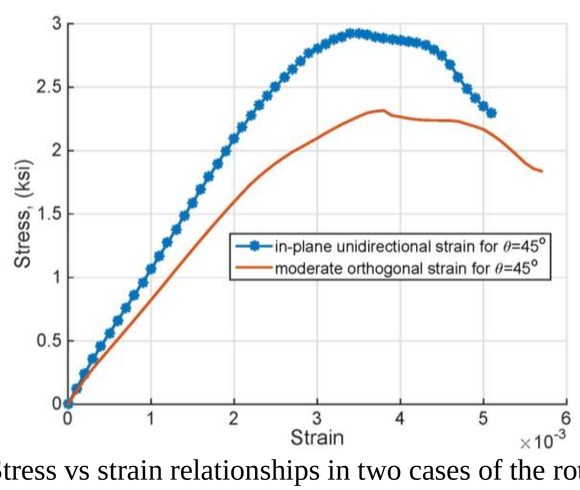

Fig. 10 – Stress vs strain relationships in two cases of the rotated unit cell

5. FEA of a masonry wall

Based on the results of the rotated unit cell with moderate orthogonal strain, the parameters of FE model are summarized in Table 4. A FE model of a diagonal tension test is developed and the results are shown in Fig. 11.

Table 4 – Effective material properties for a wall subject to diagonal tension

f_c (ksi)	G_c (kip.in)	E (ksi)	ν	f_t (ksi)	G_t (kip.in)
2.30	0.002	1100.0	0.26	0.10	0.000010

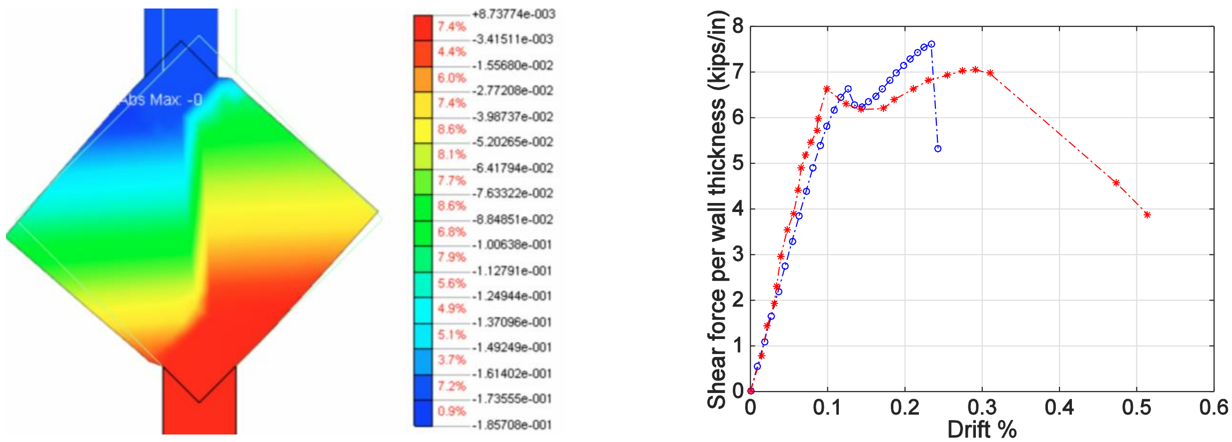

a. Horizontal displacement (in) at 0.233% drift. b. Shear stress vs drift

Fig. 11 – Results from FE model of diagonal tension test

A failure mode consisting of a vertical crack is predicted by this model. In Fig. 11b, the macroscopic response is observed to match experimental results within the error in material parameters in terms of strength. Note that, in general, a one-step homogenization by analyzing the unit cell to a reference state of strain (Eq. 19), taken from a linear elastic analysis of the wall will give better estimations of the elastic limits because the state of strain may significantly change after failure. Therefore, results can be confirmed by subsequent homogenization steps and/or by a full multiscale simulation.

6. Conclusions

A set of homogenized nonlinear material properties for masonry was developed from parameters of its constituents obtained from experiments. The elastic moduli suggest that masonry can be idealized as orthotropic material. Thus, nonlinear simulation was performed on a masonry unit cell, leading to macro stress vs macro strain relationship. The behavior of the unit cell, subjected to state of principal strain rotated 45 degrees, was investigated. Effective parameters for nonlinear analysis of masonry were inferred from the results. This model was shown to be accurate when tested against results of a diagonal tension (shear) test. The implementation of the developed model is suggested in the analysis and design of new masonry structures as well as the vulnerability assessment, retrofit and restoration of old masonry structures.

5. References

[1] Anthoine A. (1995). "Derivation of the in-plane elastic characteristics of masonry through homogenization theory." Int. J. Solids Struct. 32, 137–163.

[2] ASTM C 67 (1999). Standard Test Methods for Sampling and Testing Brick and Structural Clay Tile, American Society for Testing Materials, Pennsylvania.

[3] ASTM C 270 (2001). Standard Specification for Mortar for Unit Masonry, American Society for Testing Materials, Pennsylvania.

[4] ASTM C 1006 (2001). Standard Test Method for Splitting Tensile Strength of Masonry Units, American Society for Testing Materials, Pennsylvania.

[5] ASTM C 496 (1996). Standard Test Method for Splitting Tensile Strength of Cylindrical Concrete Specimens, American Society for Testing Materials, Pennsylvania.

[6] ASTM C 39 (2001). Standard Test Method for Compressive Strength of Cylindrical Concrete Specimens, American Society for Testing Materials, Pennsylvania.

[7] ASTM E 447 (1991). Test Methods for Compressive Strength of Laboratory Constructed Masonry Prisms, American Society for Testing Materials, Pennsylvania.

[8] ASTM E 519 (1988). Standard Test Method for Diagonal Tension (Shear) in Masonry Assemblages, American Society for Testing Materials, Pennsylvania.

[9] Berto L., Saetta A., Scotta R., Vitaliani R. (2002). “An orthotropic damage model for masonry structures.” Int. J. for Num. Methods in Eng. 55(2), 127-157. Doi:10.1002/nme.495.

[10] Briccoli Bati S., Ranocchiai G., Rovero L. (1999). “A micromechanical model for linear homogenization of brick masonry.” Materials and Structures/Matériaux et Constructions 32, 22–30.

[11] Cecchi A., Rizzi N.L. (2001). “Heterogeneous elastic solids: a mixed homogenization-rigidification technique.” Int. J. Solids Struct. 38, 29–36.

[12] Drysdale, R.G., Hamid, A.A., Baker, L.R. (1994). Masonry Structures: Behaviour and Design, Prentice Hall, N.J.

[13] Kawa M., Pietruszcza S., Shieh-Beygi B. (2008). “Limit state of brick masonry based on homogenization approach.” Int. J. Solids Struct. 45, 998–1016.

[14] Li S., Wang G. (2008) Introduction to Micromechanics and Nanomechanics. World Scientific Pub.

[15] Luciano R., Sacco E. (1997). “Homogenization technique and damage model for old masonry material.” Int. J. Solids Struct. 34 (24), 3191-3208.

[16] Luciano R., Sacco E. (1998). “Variational methods for the homogenization of periodic heterogeneous media.” Eur. J. Mech. A/Solids 17(4), 599-617.

[17] Lourenço P.B. (1996). Computational Strategies for Masonry Structures. Ph.D. Thesis, Delft University of Technology. Available from: www.civil.uminho.pt/ masonry.

[18] Mosalam K.M., Senescu R.R. (2004). Retrofitting of Unreinforced Masonry Walls using Fiber Reinforced Polymer Laminates, UCB/SEMM-2004/03.

[19] Mosalam K.M., Paulino H.H. (1997). “Evolutionary characteristic length method for smeared cracking finite element models.” Finite Element in Analysis and Design 27(1), 99-108.

[20] Pande G.N., Liang J.X., Middleton J. (1989). “Equivalent elastic moduli for brick masonry.” Comput. Geotech. 8, 243–265.

[21] Peralta N., Mosalam K., Li S. (2016). “Multiscale homogenization analysis of the effective elastic properties of masonry structures.” J. Mater. Civ. Eng., 10.1061/(ASCE)MT.1943-5533.0001561, 04016056.

[22] Pietruszczak S., Niu X. (1992). “A mathematical description of macroscopic behavior of brick masonry.” Int. J. Solids Struct. 29, 531–546.

[23] Sanchez-Palencia E. (1980). Non-Homogeneous Media and Vibration Theory. Springer, Berlin.

[24] Wang G., Li S., Nguyen H., Sitar N. (2007). “Effective elastic stiffness for periodic masonry structures via eigenstrain homogenization.” ASCE J. of Materials in Civil Eng. 19, 269–277.

[25] Zucchini A., Lourenço P.B. (2002). “A micro-mechanical model for the homogenization of masonry.” Int. J. Solids Struct. 39, 3233-3255.

[26] Zucchini, A., P.B. Lourenço P.B. (2009). “A micro-mechanical homogenisation model for masonry: Application to shear walls.” Int. J. Solids Struct. 46, 871–886.